



1 **Quantifying SO₂ oxidation pathways to atmospheric sulfate by using**
2 **stable sulfur and oxygen isotopes: laboratory simulation and field**
3 **observation**

4 Ziyan Guo^a, Keding Lu^{a*}, Pengxiang Qiu^b, Mingyi Xu^b, Zhaobing Guo^{b*}

5

6 ^a State Key Joint Laboratory of Environmental Simulation and Pollution Control,
7 State Environmental Protection Key Laboratory of Atmospheric Ozone Pollution
8 Control, College of Environmental Sciences and Engineering, Peking University,
9 Beijing, China.

10 ^b Jiangsu Key Laboratory of Atmospheric Environment Monitoring and Pollution
11 Control (AEMPC), Collaborative Innovation Center of Atmospheric Environment and
12 Equipment Technology (CIC-AEET), School of Environmental Science and
13 Engineering, Nanjing University of Information Science and Technology, Nanjing
14 210044, China

15

16 * Correspondence to: k.lu@pku.edu.cn (Keding Lu), guocumt@nuist.edu.cn
17 (Zhaobing Guo)

18



19 **Abstract.** The formation of secondary sulfate in the atmosphere remains controversial, and it is urgent
20 to seek for a new method to quantify different sulfate formation pathways. Thus, SO₂ and PM_{2.5}
21 samples were collected from 4 to 22 Dec. 2019 in Nanjing. Sulfur and oxygen isotope compositions
22 were synchronously measured to study the contribution of SO₂ homogeneous and heterogeneous
23 oxidation to sulfate. Meanwhile, the correlation of δ¹⁸O values between H₂O and sulfate from SO₂
24 oxidation by H₂O₂ and Fe³⁺/O₂ were investigated in the lab. Based on isotope mass equilibrium
25 equations, the ratios of different SO₂ oxidation pathways were calculated. The results showed that
26 secondary sulfate constituted higher than 80 % of total sulfate in PM_{2.5} during the sampling period.
27 Laboratory simulation experiments indicated that δ¹⁸O of sulfate was linearly dependent on δ¹⁸O of
28 water, and the slopes of linear curves for SO₂ oxidation by H₂O₂ and Fe³⁺/O₂ were 0.43 and 0.65,
29 respectively. The secondary sulfate in PM_{2.5} was mainly ascribed to SO₂ homogeneous oxidation by
30 OH radicals and heterogeneous oxidation by H₂O₂ and Fe³⁺/O₂. SO₂ heterogeneous oxidation was
31 generally dominant during sulfate formation, and the contribution of SO₂ heterogeneous oxidation was
32 about 52 %. Especially, SO₂ oxidation by H₂O₂ predominated in SO₂ heterogeneous oxidation reactions
33 with an average ratio around 55 %. This study provided an insight into precisely evaluating sulfate
34 formation pathways by combining stable sulfur and oxygen isotopes.

35
36
37
38
39
40



41 **1 Introduction**

42 Sulfate is one of the prevalent components of $PM_{2.5}$ (Brüggenmann et al., 2021; Huang et al., 2014;
43 Yang et al., 2023). Sulfate makes up approximately 25% of $PM_{2.5}$ mass in Shanghai, 23% in
44 Guangzhou and 10-33% in Beijing (Xue et al., 2016). The rapid sulfate formation is a crucial factor
45 determining the explosive growth of fine particles and the frequent occurrence of severe haze events in
46 China (Lin et al., 2022; Liu et al., 2020; Meng et al., 2023; Wang et al., 2021). Sulfate plays an
47 important role in tropospheric and lower stratospheric chemical and physical processes, which
48 significantly affects global climate change by scattering solar radiation and acting as cloud
49 condensation nuclei (CCN) (Gao et al., 2022; Ramanathan et al., 2001). Meanwhile, sulfate exerts a
50 significant influence on air quality and public health (Abbatt et al., 2006).

51 In the past decades, numerous attempts have been made to evaluate SO_2 oxidation pathways
52 involving in homogeneous and heterogeneous reactions. Traditionally, sulfate formation mechanisms
53 mainly include homogeneous oxidation of SO_2 by OH radicals and heterogeneous oxidation by H_2O_2 ,
54 O_3 and O_2 catalyzed by transition metal ions (TMIs) in cloud/fog water droplets. The relative
55 importance of different sulfate formation pathways is strongly dependent on oxidant concentrations,
56 occurrence of fog/cloud events and pH of aqueous phase (Seinfeld et al., 2016; Kuang et al., 2022; Oh
57 et al., 2023). Generally, SO_2 homogeneous oxidation by OH and heterogeneous oxidation by H_2O_2 are
58 considered the most important pathways for sulfate production on the global scale (Seinfeld et al.,
59 2006). The photochemical reactivity during the winter in Beijing has been found to be relatively high,
60 which favors the formation of reactive species such as OH radicals and H_2O_2 , thereby facilitating SO_2
61 oxidation (Zhang et al., 2020). Xue et al. (2014) suggested that SO_2 oxidation by O_3 and H_2O_2 in
62 aqueous phase contributed to the majority of total sulfate production. Liu et al. (2020) proposed that
63 S(IV) oxidation by H_2O_2 in aerosol water could be an important pathway considering the ionic strength
64 effect. He et al. (2018) found that the contribution of SO_2 oxidation by H_2O_2 could reach 88 % during
65 Beijing haze period. Ye et al. (2018) observed that SO_2 oxidation rate by H_2O_2 was 2-5 times faster
66 than the summed rate of the other three oxidation pathways. As a result, actual contribution of SO_2
67 oxidation by H_2O_2 during the winter might be underestimated in previous studies.

68 In addition, the presence of NO_2 was obviously favorable for SO_2 oxidation under the conditions of
69 high RH and NH_3 . NH_3 can promote the hydrolysis of NO_2 dimers to HONO and result in more sulfate



70 formation on particle surface in humid conditions. However, this conclusion was doubted by Liu et al.
71 (2017) who believed that the reaction on actual fine particles with pH at 4.2 was too slow to account
72 for sulfate formation. Li et al. (2020) deemed that SO₂ oxidation by NO₂ might not be a major
73 oxidation pathway in China. Furthermore, GEOS-Chem modeling study suggested that NO₂ oxidation
74 contributed less than 2% of total sulfate production. It is found that TMI pathway was very important in
75 highly polluted regions, and the contribution of metal-catalyzed SO₂ oxidation to sulfate was as high as
76 49±10% in haze. Wang et al. (2021) also argued that SO₂ oxidation by TMI on aerosol surface could be
77 the dominant sulfate formation pathway. They found that manganese-catalyzed oxidation of SO₂
78 contributed 69.2±5.0% in sulfate production. Overall, the mechanisms for sulfate rapid growth remain
79 unclear and controversial. Therefore, sulfate formation pathways via SO₂ oxidation need to be further
80 explored, and it is urgent to develop a new method to quantify different sulfate formation processes.

81 Generally, sulfur isotopes allow for investigating SO₂ oxidation processes in the atmosphere because
82 of distinctive isotope fractionation associated with different oxidation reactions (Harris et al., 2013).
83 Harris et al. (2012) presented sulfur isotope fractionation factors of SO₂ oxidation by OH, O₃/H₂O₂ and
84 iron catalysis were 1.0087, 1.0167 and 0.9905, respectively. Besides, the observed sulfur isotope
85 fractionation of SO₂ oxidation by H₂O₂ and O₃ appeared to be no significant difference. Therefore, the
86 results were particularly useful to determine the importance of transition metal-catalyzed oxidation
87 pathway compared to other oxidation pathways. However, other main oxidation pathways of SO₂ could
88 not be distinguished only based on stable sulfur isotope determination.

89 Oxygen isotope ratio ($\delta^{18}\text{O}$) can be used to deduce sulfate formation processes due to those different
90 SO₂ oxidation pathways affect oxygen isotope of product sulfate differently. Especially,
91 mass-independent fractionation signals (nonzero $\Delta^{17}\text{O}$, where $\Delta^{17}\text{O}=\delta^{18}\text{O}-0.52\times\delta^{17}\text{O}$) of oxygen
92 isotopes in sulfate are usually adopted to investigate the contributions of different SO₂ oxidation
93 pathways. This method can identify the contribution of SO₂+O₃ pathway when high $\Delta^{17}\text{O}$ (>3‰) is
94 measured in sulfate. However, there is presence of obvious uncertainty when interpreting the sulfate
95 with low $\Delta^{17}\text{O}$ value (<1‰). Unfortunately, most sulfate samples in the atmosphere show $\Delta^{17}\text{O}<1\text{‰}$,
96 suggesting a limited contribution of SO₂+O₃ pathway during sulfate formation. It is noteworthy that the
97 contribution of SO₂+H₂O₂ pathway and TMI pathway is unclear if solely using $\Delta^{17}\text{O}$ (Li et al., 2020).
98 Holt et al. (1982) found oxygen isotope was a valuable and complementary method to determine



99 probable mechanisms of SO₂ oxidation to sulfate in the atmosphere. This provides us an insight into
100 precisely evaluating sulfate formation pathways by combining oxygen and sulfur isotopes.

101 In this contribution, PM_{2.5} samples were collected from 4 to 22 Dec. 2019 in Nanjing region. Sulfur
102 and oxygen isotope compositions in sulfate were measured to study the contribution of SO₂
103 homogeneous and heterogeneous oxidation during sulfate formation. In addition, the linear
104 relationships of δ¹⁸O values between H₂O and sulfate from SO₂ oxidation by H₂O₂ and Fe³⁺/O₂ were
105 synchronously investigated in the lab. Based on sulfur and oxygen isotope mass equilibrium equations,
106 the ratios of different SO₂ oxidation pathways during the sampling period were calculated. The study
107 aims to seek for a novel method to quantify different SO₂ oxidation processes with sulfur and oxygen
108 isotopes.

109 **2 Materials and methods**

110 2.1 Sampling location

111 PM_{2.5} and SO₂ in the atmosphere were sampled from 4 to 22 Dec. 2019 in Nanjing, China. The
112 sampling site was located at the roof of the library in Nanjing University of Information Science &
113 Technology (NUIST, 32.1 °N, 118.5 °E), which is depicted in Fig. 1. The sampling location is at the
114 side of Ningliu Road and closely next to Nanjing chemical industry park. There is presence of some
115 large-scale chemical enterprises such as Nanjing steel plant, Nanjing thermal power plants and Nanjing
116 petrochemical company, which inevitably release lots of SO₂ and iron metal into the atmosphere.

117 2.2 PM_{2.5} and SO₂ Samples collection

118 PM_{2.5} and SO₂ were sampled using a modified JCH-1000 sampler (Juchuang Co., Qingdao) with a
119 flow rate of 1.05 m³ min⁻¹ from 8 am to 8 pm from 4 to 22 Dec. 2019. PM_{2.5} and SO₂ were collected
120 with quartz filter (203×254 mm, Munktell, Sweden) and glass fiber filter (203×254 mm, Tisch
121 Environment INC, USA), respectively. The filters were incinerated in a muffle furnace at 450 °C for 2h
122 and then preserved in the desiccators at room temperature. The glass fiber filters were firstly soaked in
123 2% K₂CO₃ and 2% glycerol solution for 2h and dried in DGG-9070A electric oven. SO₂ can be
124 changed into sulfite immediately during the sampling.

125 2.3 Extractions of water-soluble sulfate

126 PM_{2.5} sample filters were shredded and soaked in 400 mL of Milli-Q (18 MΩ) water for extractions



127 of water-soluble sulfate. Filters were then isolated from solutions by centrifugation and water-soluble
128 sulfate was precipitated as BaSO₄ by adding 1 mol L⁻¹ BaCl₂. After the filtration with 0.22 μm acetate
129 membrane, BaSO₄ precipitate was rinsed with Milli-Q water to remove Cl⁻. Finally, BaSO₄ powders
130 were calcined at 800 °C for 2h to obtain high purity BaSO₄. In addition, a small amount of H₂O₂
131 solution was added to oxidize sulfite to sulfate.

132 2.4 Laboratory simulation of SO₂ oxidation by H₂O₂ and Fe³⁺/O₂

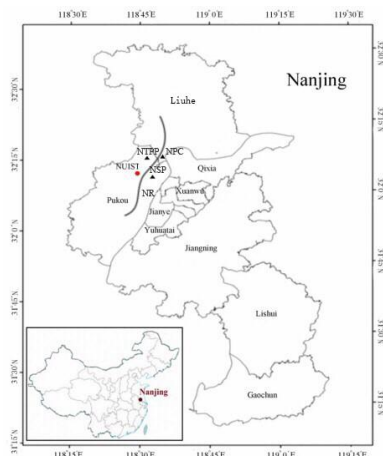
133 For SO₂ oxidation by H₂O₂, 30 mL min⁻¹ Ar was firstly introduced into three kinds of different water
134 about 30 min to drive out air. Sulfate was produced by adding 10 mL H₂O₂ dilute solution (0.1 mL 30%
135 H₂O₂ in 50 mL water) to SO₂ in the reaction chamber at 10 °C. H₂O₂ solution was agitated vigorously
136 for 1min before admission of air. For Fe³⁺ catalyzed oxidation of SO₂, 2 mL min⁻¹ SO₂ and 2 mL min⁻¹
137 O₂ were simultaneously put into Fe³⁺ dilute solution at 10 °C. Then, 10 mL 1 mL min⁻¹ BaCl₂ was
138 added to prepare BaSO₄. Oxygen isotope compositions of product sulfate and three kinds of water were
139 measured to study their linear relationships.

140 2.5 Sulfur and oxygen isotope determination

141 Sulfur isotope compositions in sulfate were analyzed using Elemental analyzer (EA, Flash 2000,
142 Thermo) and isotope mass spectrometer (IRMS, Delta V Plus, Finningan). High-purity BaSO₄ was
143 converted into SO₂ in EA in the presence of Cu₂O. SO₂ from EA was ionized and δ³⁴S value was
144 measured using IRMS. For the determination of δ¹⁸O, BaSO₄ pyrolysis was conducted in graphite
145 furnace at 1450 °C, and δ¹⁸O value was obtained in CO produced from the pyrolysis at continuous-flow
146 mode. The results of δ³⁴S and δ¹⁸O were with respect to international standard V-CDT and V-SMOW,
147 and the accuracy were better than ±0.2‰ and ±0.3‰, respectively.

148 3 Results and discussion

149 3.1 Concentrations of PM_{2.5}, sulfate and SO₂



150

151

Fig.1. Sampling site of NUIST in Nanjing, China. NSP: Nanjing steel plants; NTPP: Nanjing thermal power plants; NPC: Nanjing petrochemical company; NR: Ningliu Road.

152

153

154

155

156

157

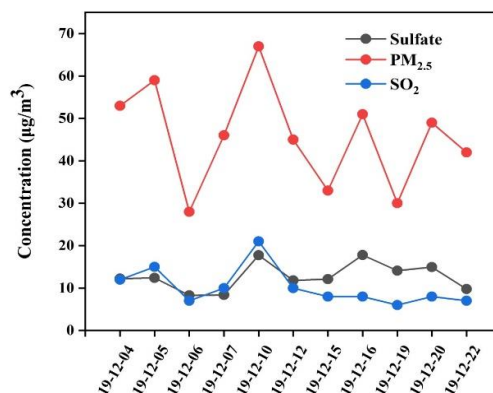
158

159

160

161

As described in Fig. 2, the mass concentrations of $PM_{2.5}$, SO_4^{2-} and SO_2 during the period from 4 to 22 Dec. 2019 in NUIST changed from 28.1 to 67.0 $\mu g m^{-3}$, 8.3 to 17.8 $\mu g m^{-3}$ and 6.2 to 20.9 $\mu g m^{-3}$ with an average and standard deviation at $45.7 \pm 12.1 \mu g m^{-3}$, $12.7 \pm 3.3 \mu g m^{-3}$ and $10.2 \pm 4.4 \mu g m^{-3}$, respectively. It can be observed that $PM_{2.5}$ average concentration was about 1.3 times of the First Grade National Ambient Air Quality Standard ($35 \mu g m^{-3}$) and beyond the safety standard of World Health Organization ($10 \mu g m^{-3}$). The photochemical reactivity during the winter in Beijing has been found to be relatively high (Zhang et al., 2020), which facilitates the formation of some photooxidants. The relatively clean days during the sampling period indicates the importance of photoinduced oxidation of SO_2 .



162



163 **Fig. 2.** The concentrations of $\text{PM}_{2.5}$, SO_4^{2-} and SO_2 .

164 Meanwhile, the change trends of $\text{PM}_{2.5}$, SO_4^{2-} and SO_2 concentrations were found to be basically the
165 same during the sampling period, suggesting sulfate was mainly from SO_2 oxidation. Especially, $\text{PM}_{2.5}$,
166 SO_4^{2-} and SO_2 concentrations increased to the maximum values on 10 Dec.. It is noted that NO_2 and
167 CO concentrations were 85 and $1.60 \mu\text{g m}^{-3}$ on 10 Dec., which were also the maximum values during
168 the sampling period. High CO concentration indicates that the pollution was mainly from local
169 emissions. However, O_3 concentration on 10 Dec. was the minimum value at $24 \mu\text{g m}^{-3}$, which
170 preliminarily indicates that SO_2 oxidation by NO_2 might be a major pathway in sulfate formation.
171 Previous studies showed that SO_2 oxidation by NO_2 in aerosol water dominated heterogeneous sulfate
172 formation during wintertime at neutral aerosol pH (Wang et al., 2016; Cheng et al., 2016). However,
173 subsequent studies showed that the calculated aerosol pH was in the range of 4.2~4.7, and the
174 reactions between SO_2 and NO_2 during this pH range were too slow to produce sulfate. Taking into
175 account low aerosol pH in Nanjing region, we suggested that SO_2 oxidation by NO_2 was not a
176 dominant pathway for sulfate formation during the sampling period.

177 In contrast, $\text{PM}_{2.5}$, SO_4^{2-} and SO_2 concentrations were observed to be at the minimum values On 6
178 Dec.. Similarly, NO_2 and CO concentrations were also at the minimum of 36 and 0.6 mg m^{-3} ,
179 respectively. However, O_3 concentration on 6 Dec. was the maximum at $50 \mu\text{g m}^{-3}$. Besides, the rate of
180 SO_2 oxidation with O_3 becomes fast only when $\text{pH}>5$, the reaction rate of SO_2 with O_3 is one hundredth
181 of those with H_2O_2 or TMI when $\text{pH}<5$. Therefore, pH values of actual fine particles at 4~5 in Nanjing
182 could markedly restrain SO_2 oxidation by O_3 . The lowest SO_4^{2-} concentration on 6 Dec. further
183 demonstrated that SO_2 oxidation by O_3 played an insignificant role in sulfate formation.

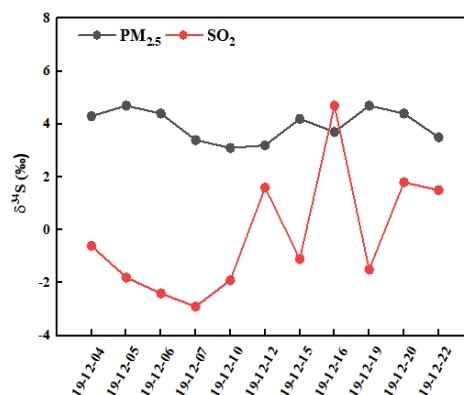
184 Generally, aqueous-phase oxidation is deemed to be a main process of sulfate formation in
185 atmospheric environment. Shao et al. (2018) believed that heterogeneous sulfate production on aerosols
186 occurred when relative humidity (RH) was higher than 50 %. The RH values of the atmosphere ranging
187 from 50.7 to 88.9% during the sampling period indicated that sulfate formation was closely related to
188 the heterogeneous oxidation of SO_2 .

189 3.2 Sulfur isotope compositions in sulfate and SO_2

190 It can be observed from Fig. 3 that the values of $\delta^{34}\text{S-SO}_4^{2-}$ were generally higher compared to those
191 of $\delta^{34}\text{S-SO}_2$ during the sampling period except that on 16 Dec.. The $\delta^{34}\text{S-SO}_4^{2-}$ values ranged from 3.1



192 to 4.7‰ with an average and standard deviation at 4.0 ± 0.6 ‰, while $\delta^{34}\text{S}\text{-SO}_2$ values changed from -2.9
193 to 4.7‰ with an average and standard deviation at -0.2 ± 2.3 ‰. The discrepancy between the values of
194 $\delta^{34}\text{S}\text{-SO}_4^{2-}$ and $\delta^{34}\text{S}\text{-SO}_2$ was mainly related to sulfur isotope fractionation effect during SO_2 oxidation
195 to secondary sulfate.



196
197

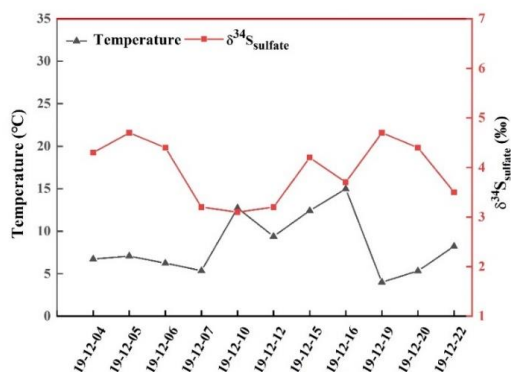
Fig. 3. Sulfur isotope compositions in sulfate and SO_2 .

198 It is noteworthy that the values of $\delta^{34}\text{S}\text{-SO}_4^{2-}$ were similar to that in $\text{PM}_{2.5}$ with an average at 4.2‰
199 during Youth Olympic Games in Aug. 2014 in Nanjing (Guo et al., 2016). However, the average value
200 of $\delta^{34}\text{S}\text{-SO}_4^{2-}$ during the sampling period was lower than 5.6‰ in Nanjing during a typical haze event
201 from 21 Dec. 2015 to 1 Jan. 2016 (Guo et al., 2019). The higher $\delta^{34}\text{S}$ values of sulfate in haze was
202 possibly ascribed to SO_2 heterogeneous oxidation, which typically enriched heavy sulfur isotope in
203 sulfate. In this study, the average concentrations of $\text{PM}_{2.5}$ was $45.7 \mu\text{g m}^{-3}$, indicating a not heavily
204 polluted time interval. Besides, the relatively high temperature during the sampling period was
205 favorable for photochemical reactions and OH radicals formation. As a result, the contribution of SO_2
206 homogenous oxidation increased during sulfate formation, which enriched light sulfur isotope
207 compared to that in haze. Han et al. (2017) determined $\delta^{34}\text{S}$ values in Beijing $\text{PM}_{2.5}$ with an average at
208 6.0‰. It is observed that there existed a regional difference in $\delta^{34}\text{S}\text{-SO}_4^{2-}$ values. The $\delta^{34}\text{S}\text{-SO}_4^{2-}$ in
209 Nanjing was generally lower than that in Beijing. The discrepancy of $\delta^{34}\text{S}\text{-SO}_4^{2-}$ illustrated different
210 sulfur sources and SO_2 oxidation pathways in these regions. In addition, $\delta^{34}\text{S}\text{-SO}_4^{2-}$ values presented a
211 seasonal change. $\delta^{34}\text{S}$ values in Beijing aerosol sulfate varied from 3.4 to 7.0‰ with an average of
212 5.0‰ in summer and from 7.1 to 11.3‰ with an average of 8.6‰ in winter. Generally, the
213 homogeneous oxidation of SO_2 dominated in summer compared to that in winter due to strong solar



214 irradiation (Han et al., 2016). SO₂ oxidation might lead to sulfur isotope fractionation, which was
 215 mainly attributed to equilibrium or kinetic discrimination between SO₂ and sulfate. The influence of
 216 different oxidants on sulfur isotope fractionation needed to be further investigated.

217 Fig.4 presents the relationship between δ³⁴S-SO₄²⁻ and atmospheric temperature during the
 218 sampling period. It can be observed that there existed an obviously negative correlation. The higher
 219 temperature generally corresponded to the lower δ³⁴S-SO₄²⁻. This is mainly ascribed to kinetic effect of
 220 sulfur isotope fractionation during SO₂ oxidation. At high temperature, more OH radicals were
 221 produced and the contribution of SO₂ homogeneous oxidation increased. It is reported that sulfur
 222 isotope fractionation about SO₂ was -9‰ for homogeneous oxidation process (Tanaka et al., 1994).
 223 Therefore, low δ³⁴S value in sulfate at high temperature was chiefly due to elevated SO₂ homogeneous
 224 oxidation.



225
 226 **Fig. 4.** The relationship between δ³⁴S-SO₄²⁻ and atmospheric temperature.

227 3.3 Sulfur isotope fractionation during SO₂ oxidation

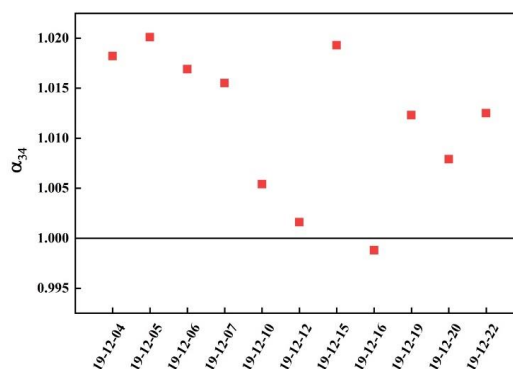
228 The secondary sulfate was generally from SO₂ homogeneous and heterogeneous oxidation (Seinfeld
 229 et al., 2016). The homogeneous and heterogeneous oxidation of SO₂ led to sulfur isotope fractionation,
 230 which is described by using fractionation coefficient (α)

$$\alpha = \frac{\frac{\delta^{34}\text{S}_{\text{SO}_4^{2-}}}{10^3} + 1}{\frac{\delta^{34}\text{S}_{\text{SO}_2} + 1}{10^3}} \quad (1)$$

231
 232 Sulfate enriched heavy sulfur isotope (α>1) during SO₂ heterogeneous oxidation due to the presence
 233 of isotope equilibrium fractionation and kinetic fractionation. However, sulfate enriched light sulfur



234 isotope ($\alpha < 1$) during SO_2 homogeneous oxidation for this process was only related to kinetic
235 fractionation. As described in Fig. 5, α values ranged from 0.9988 to 1.0201, indicating there existed
236 SO_2 homogeneous and heterogeneous oxidation during the sampling period. α value was at the
237 minimum of 0.9988 on 16 Dec., which showed SO_2 homogeneous oxidation played a crucial role.



238

239

Fig. 5. Sulfur isotope fractionation coefficients during SO_2 oxidation.

240 It is reported that sulfur isotope fractionations during SO_2 heterogeneous and homogeneous oxidation
241 to sulfate were 16.5‰ and -9‰, respectively (Tanaka et al., 1994). Consequently, the contribution of
242 SO_2 heterogeneous and homogeneous oxidation to sulfate could be calculated by sulfur isotope mass
243 equilibrium equations (2) and (3).

$$244 \quad \delta^{34}\text{S}_{\text{SO}_2} + 16.5x - 9y = \delta^{34}\text{S}_{\text{SO}_4^{2-}} \quad (2)$$

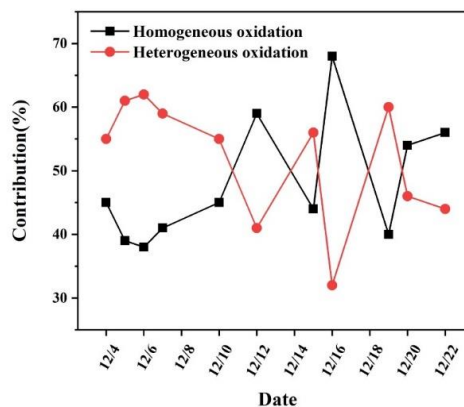
$$245 \quad x + y = 1 \quad (3)$$

246 where x and y represent the contribution of SO_2 heterogeneous and homogeneous oxidation,
247 respectively.

248 It is observed from Fig. 6 that the contribution of SO_2 heterogeneous oxidation markedly fluctuated
249 ranging from 31.4 to 62.0% with an average and standard deviation at $51.6 \pm 0.1\%$, which indicated that
250 SO_2 heterogeneous oxidation was generally dominant during sulfate formation. He et al. (2018)
251 presented the observations of oxygen-17 excess of $\text{PM}_{2.5}$ sulfate collected in Beijing haze from Oct.
252 2014 to Jan. 2015, and found the contribution of heterogeneous sulfate production was about 41~54%
253 with a mean of $48 \pm 5\%$. The contribution of SO_2 heterogeneous oxidation reached high-level during 5-7
254 Dec. and on 19 Dec., which was closely related to the temperature of the atmosphere. The low
255 temperature about 5 °C in these days was favorable for SO_2 dissolution in water and further oxidized to



256 sulfate by the oxidants. On 16 Dec., the contribution of SO₂ heterogeneous oxidation was the minimum
257 at 31.4%. The highest temperature of 15 °C on 16 Dec. restrained SO₂ solubility in aqueous solution
258 and produced lots of gaseous oxidants such as OH to promote SO₂ homogeneous oxidation.



259

260 **Fig. 6.** The contributions of SO₂ heterogeneous and homogeneous oxidation to sulfate.

261 Overall, the temperature was an important factor in controlling SO₂ oxidation pathways. High
262 temperature facilitated kinetic fractionation of sulfur isotope during SO₂ oxidation to sulfate, thereby
263 decreasing $\delta^{34}\text{S}$ value in sulfate. In addition, it was not found to be positive correlation between the
264 contribution of SO₂ heterogeneous oxidation and O₃ or NO₂ concentration. This also further
265 demonstrated that SO₂ oxidation by O₃ and NO₂ were not main pathways during the sampling period.
266 Consequently, we mainly focused on SO₂ heterogeneous oxidation by H₂O₂ and Fe³⁺/O₂ in the
267 following study.

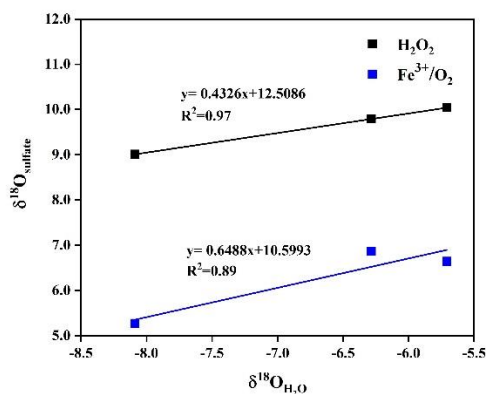
268 3.4 The correlation of $\delta^{18}\text{O}$ between H₂O and SO₄²⁻ from SO₂ oxidation by H₂O₂ and Fe³⁺/O₂

269 It is known that SO₂ rapidly equilibrates with ambient water for very high molar ratio of H₂O to SO₂
270 in the atmosphere. As a result, $\delta^{18}\text{O}$ of SO₂ is dynamically controlled by $\delta^{18}\text{O}$ of water and $\delta^{18}\text{O}$ of SO₂
271 has no obvious effect on $\delta^{18}\text{O}$ of sulfate formed by different oxidation pathways. Meanwhile, sulfate is
272 very stable with respect to O atom exchange with ambient water. Consequently, $\delta^{18}\text{O}$ can be adopted to
273 distinguish SO₂ oxidation processes due to that $\delta^{18}\text{O}$ of product sulfate reflected the distinctive signals
274 of different oxidants.

275 In this manuscript, we firstly studied SO₂ heterogeneous oxidation by H₂O₂ and Fe³⁺/O₂ in the lab,
276 which aims to make clear the relationship of $\delta^{18}\text{O}$ between product sulfate and water at 10 °C. It can be



277 observed from Fig. 7 that $\delta^{18}\text{O}$ of sulfate was linearly dependent on $\delta^{18}\text{O}$ of water, and the slope of
278 linear curve for H_2O_2 oxidation approximates a ratio of 0.43, indicating that the isotopy of about two of
279 four oxygen atoms in sulfate was controlled by $\delta^{18}\text{O}$ of water. The other two oxygen atoms were from
280 H_2O_2 molecules, whose O-O bonds remained intact during SO_2 oxidation. In addition, we noted from
281 Fig. 7 that the slope of linear curve for $\text{Fe}^{3+}/\text{O}_2$ oxidation was 0.65, which represented that the isotopy
282 of about three of four oxygen atoms in sulfate was related to $\delta^{18}\text{O}$ of water. A 3/4 control of sulfate
283 oxygens by water is also characteristic of heterogeneous oxidation mechanisms in which HSO_3^-
284 isotopically equilibrated with water prior to significant oxidation to SO_4^{2-} . The other one oxygen atom
285 in sulfate was from O_2 . The higher slope suggested a higher dependence of $\delta^{18}\text{O}$ of sulfate on $\delta^{18}\text{O}$ of
286 water during SO_2 heterogeneous oxidation by $\text{Fe}^{3+}/\text{O}_2$. The difference of the slope for different SO_2
287 heterogeneous oxidation processes provides us a novel method to distinguish SO_2 oxidation pathways.



288

289 **Fig.7.** The correlation of $\delta^{18}\text{O}$ between H_2O and SO_4^{2-} from SO_2 oxidation by H_2O_2 and $\text{Fe}^{3+}/\text{O}_2$,
290 respectively.

291 3.5 $\delta^{18}\text{O}$ - SO_4^{2-} in $\text{PM}_{2.5}$ and SO_2 main oxidation pathways

292 As depicted in Fig. 8, $\delta^{18}\text{O}$ values of sulfate in $\text{PM}_{2.5}$ ranged from 11.09 to 12.93‰ with an average
293 and standard deviation of 12.35 ± 0.68 ‰. $\delta^{18}\text{O}$ values of sulfate focused on a narrow scope except those
294 on 5 and 22 Dec.. It should be pointed out $\delta^{18}\text{O}$ value of secondary sulfate was a comprehensive result
295 from different SO_2 oxidation processes. Sulfate in $\text{PM}_{2.5}$ usually consisted of primary sulfate and
296 secondary sulfate. The $\delta^{18}\text{O}$ value of primary sulfate is about 38 ‰, which is significantly higher than
297 those of secondary sulfates. The contribution of primary and secondary sulfate in the atmosphere can

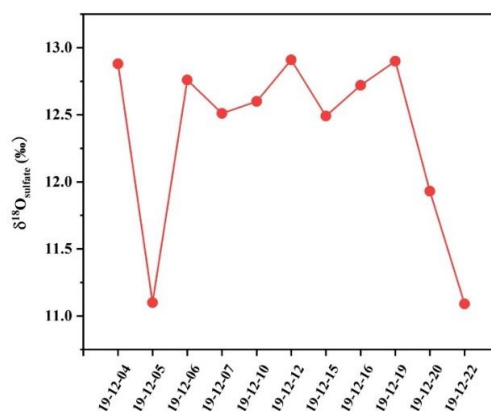


298 be calculated by oxygen isotope mass equilibrium equation (4) (Ben et al., 1982).

$$299 \quad \delta^{18}\text{O}_{\text{PM}_{2.5}} = \delta^{18}\text{O}_{\text{PS}} \times (1 - f_{\text{SS}}) + \delta^{18}\text{O}_{\text{SS}} \times f_{\text{SS}} \quad (4)$$

300 where $\delta^{18}\text{O}_{\text{PM}_{2.5}}$, $\delta^{18}\text{O}_{\text{PS}}$ and $\delta^{18}\text{O}_{\text{SS}}$ mean $\delta^{18}\text{O}$ values of $\text{PM}_{2.5}$, primary sulfate and secondary sulfate,

301 respectively; f_{SS} is the contribution of secondary sulfate in $\text{PM}_{2.5}$.



302

303 **Fig.8.** $\delta^{18}\text{O}$ values of sulfate in $\text{PM}_{2.5}$ during the sampling period.

304 Table 1 shows the contribution of primary sulfate and secondary sulfate in $\text{PM}_{2.5}$ during the sampling
 305 period. It can be observed that the majority of sulfate in $\text{PM}_{2.5}$ was secondary sulfate. Secondary sulfate
 306 appears to constitute from 80.0 to 86.1% of the total sulfate. As discussed above, secondary sulfate was
 307 mainly ascribed to SO_2 homogeneous oxidation by OH radicals and heterogeneous oxidation by H_2O_2
 308 and $\text{Fe}^{3+}/\text{O}_2$. Therefore, it is admirable to quantitatively describe these formation pathways of secondary
 309 sulfate in $\text{PM}_{2.5}$.

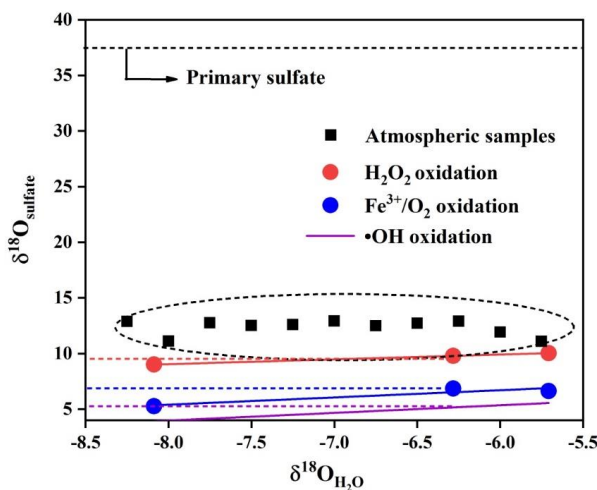
310 **Table 1** The contribution of primary sulfate and secondary sulfate in $\text{PM}_{2.5}$.

Sampling time	Primary sulfate (%)	Secondary sulfate (%)
4 Dec.	10.9-23.7	76.3-89.1
5 Dec.	4.6-18.2	81.8-95.4
6 Dec.	10.6-23.3	76.7-89.4
7 Dec.	9.6-22.5	77.5-90.4
10 Dec.	10.0-22.8	77.2-90.0
12 Dec.	11.1-23.8	76.2-89.9
15 Dec.	9.6-22.5	77.5-90.4



16 Dec.	11.9-23.6	76.4-88.1
19 Dec.	11.0-23.7	76.3-89.0
20 Dec.	7.7-20.8	79.2-92.3
22 Dec.	4.5-18.1	79.1-95.5

311 It is noteworthy that there exists a linear relationship between $\delta^{18}\text{O}$ values in water and primary
 312 sulfate or secondary sulfate from different oxidation pathways (Fig. 9), which can be described by the
 313 equations (5)-(8). $\delta^{18}\text{O}$ values of sulfate in atmospheric samples consist of those of primary sulfate and
 314 secondary sulfate. Considering the contribution of primary sulfate and secondary sulfate as well as $\delta^{18}\text{O}$
 315 water is about -6.2‰ in Nanjing region, we can calculate the ratios of different SO_2 oxidation pathways
 316 at 10 °C via oxygen isotope mass equilibrium equations (9)-(11), and the corresponding results are
 317 depicted in Table 2.



318
 319 **Fig.9.** The correlation between $\delta^{18}\text{O}$ values in water and sulfate in $\text{PM}_{2.5}$.

320
$$\delta^{18}\text{O}_{\text{sulfate}} = 0.06 \times \delta^{18}\text{O}_{\text{water}} + 38 \text{‰ (PS)} \text{ (Holt et al., 1983)} \quad (5)$$

321
$$\delta^{18}\text{O}_{\text{sulfate}} = 0.69 \times \delta^{18}\text{O}_{\text{water}} + 9.5 \text{‰ (SS, OH)} \text{ (Holt et al., 1983)} \quad (6)$$

322
$$\delta^{18}\text{O}_{\text{sulfate}} = 0.65 \times \delta^{18}\text{O}_{\text{water}} + 10.6 \text{‰ (SS, Fe}^{3+}/\text{O}_2) \text{ (this study)} \quad (7)$$

323
$$\delta^{18}\text{O}_{\text{sulfate}} = 0.43 \times \delta^{18}\text{O}_{\text{water}} + 12.5 \text{‰ (SS, H}_2\text{O}_2) \text{ (this study)} \quad (8)$$

324
$$\delta^{18}\text{O}_{\text{PM}_{2.5}} = \delta^{18}\text{O}_{\text{PS}} \times f_{\text{PS}} + (\delta^{18}\text{O}_{\text{SS-OH}} \times f_{\text{SS-OH}} + \delta^{18}\text{O}_{\text{SS-Fe}^{3+}/\text{O}_2} \times f_{\text{SS-Fe}^{3+}/\text{O}_2} + \delta^{18}\text{O}_{\text{SS-H}_2\text{O}_2} \times f_{\text{SS-H}_2\text{O}_2}) \times f_{\text{SS}} \quad (9)$$

325
$$f_{\text{PS}} + f_{\text{SS}} = 1 \quad (10)$$



326
$$f_{SS-OH} + f_{SS-Fe^{3+}/O_2} + f_{SS-H_2O_2} = 1 \quad (11)$$

327 where $\delta^{18}O_{PM_{2.5}}$ and $\delta^{18}O_{PS}$ are $\delta^{18}O$ values of total sulfate and primary sulfate in $PM_{2.5}$; $\delta^{18}O_{SS-OH}$,
 328 $\delta^{18}O_{SS-Fe^{3+}/O_2}$ and $\delta^{18}O_{SS-H_2O_2}$ are $\delta^{18}O$ values of secondary sulfate from SO_2 oxidation by OH radical,
 329 Fe^{3+}/O_2 and H_2O_2 , respectively; f_{PS} and f_{SS} are the contribution of primary and secondary sulfate; f_{SS-OH} ,
 330 f_{SS-Fe^{3+}/O_2} and $f_{SS-H_2O_2}$ are the contribution of secondary sulfate from SO_2 oxidation by OH radicals,
 331 Fe^{3+}/O_2 and H_2O_2 , respectively.

332 Unlike heavily polluted days with reduced solar irradiation, the photochemical reactivity could
 333 remain high in relatively clean days during the observation period because of intense solar irradiation.
 334 As a result, some photochemical reactive species such as OH radicals and H_2O_2 are deemed to be the
 335 major oxidants for sulfate formation. It is observed from Table 2 that the ratio of SO_2 oxidation by OH
 336 radicals ranged from 38 to 68% with an average and standard deviation at $48 \pm 9.7\%$. The ratio reached
 337 the maximum of 68% on 16 Dec., which is mainly ascribed to the highest temperature of 15 °C during
 338 the sampling period. The photochemical reactions are favorable for producing more OH radicals. In
 339 contrast, the ratio of SO_2 oxidation by OH radicals decreased to the minimum on 6 Dec. due to the low
 340 temperature.

341 **Table 2** The ratio of SO_2 different oxidation pathways to sulfate.

Sampling time	OH oxidation ratio	H_2O_2 oxidation ratio	Fe^{3+}/O_2 oxidation ratio	Percentage of H_2O_2 oxidation in SO_2 heterogeneous reactions (%)
4 Dec.	0.45	0.27	0.28	49
5 Dec.	0.39	0.24	0.37	40
6 Dec.	0.38	0.24	0.38	39
7 Dec.	0.41	0.25	0.34	43
10 Dec.	0.45	0.27	0.28	49
12 Dec.	0.59	0.30	0.11	74
15 Dec.	0.44	0.26	0.30	47
16 Dec.	0.68	0.26	0.06	80
19 Dec.	0.4	0.25	0.35	41
20 Dec.	0.54	0.31	0.15	67



22 Dec. 0.56 0.32 0.12 72

342

343 SO₂ heterogeneous oxidation was relatively dominant during the sampling period. It is known that
344 SO₂ oxidation by H₂O₂ and Fe³⁺/O₂ are the most important pathways during the heterogeneous
345 oxidation. From table 2, the percentage of sulfate from SO₂ oxidation by H₂O₂ in total secondary
346 sulfate from SO₂ heterogeneous oxidation reactions varied from 39 to 80% with an average and
347 standard deviation at 54.6±15.5%, indicating that H₂O₂ oxidation predominated during SO₂
348 heterogeneous reactions. In addition, there existed an obviously positive correlation between the ratio
349 of SO₂ oxidation by H₂O₂ and OH radicals, which was chiefly attributed to photochemical reactions.
350 The relatively strong solar irradiation on 16 Dec. resulted in the maximum ratio of 80% about H₂O₂
351 oxidation in SO₂ heterogeneous reactions. The sampling site is near to Nanjing steel plant. As
352 companion emitters, Fe³⁺ are present in much higher concentrations than that in other areas. It is
353 believed that SO₂ oxidation by O₂ in the presence of Fe³⁺ was important in the areas where the
354 concentrations of SO₂ and Fe³⁺ were high. This inevitably resulted in high Fe³⁺/O₂ oxidation ratio in
355 SO₂ heterogeneous oxidation reactions.

356 **4 Conclusions**

357 There was no serious PM_{2.5} pollution during the sampling period. The secondary sulfate constitutes
358 from about 80.0 to 86.1% of total sulfate in PM_{2.5}. SO₂ oxidation by O₃ and NO₂ played an
359 insignificant role in sulfate formation. The secondary sulfate was mainly ascribed to SO₂ homogeneous
360 oxidation by OH radicals and heterogeneous oxidation by H₂O₂ and Fe³⁺/O₂. Compared to
361 homogeneous oxidation, SO₂ heterogeneous oxidation was generally dominant during sulfate formation.
362 The contribution of SO₂ heterogeneous oxidation was about 52%. SO₂ oxidation by H₂O₂ predominated
363 in SO₂ heterogeneous oxidation reactions and the average ratio of which reached 55%.

364

365 **Author contribution**

366 Ziyang Guo analyzed the data and wrote the original draft. Keding Lu designed the methodology and
367 administrated the project. Pengxiang Qiu and Mingyi Xu performed the data collection. Zhaobing Guo
368 reviewed and revised the paper

369 **Competing interests**



370 The authors declare that they have no known competing interests or personal relationships that could
371 have appeared to influence the work reported in this paper.

372 **Acknowledgement**

373 We gratefully acknowledge the financial supports from the National Natural Science Foundation of
374 China (Nos. 41873016, 51908294, and 21976006), the National Science Fund for Distinguished Young
375 Scholars (No. 22325601).

376

377



378 **References**

- 379 Abbatt, J., Benz, S., Cziczo, D., Kanji, Z., Lohmann, U., and Mohler, O.: Solid ammonium sulfate
380 aerosols as ice nuclei: a pathway for cirrus cloud formation, *Science*, 313, 1770-1773,
381 <https://doi.org/10.1126/science.1129726>, 2006.
- 382 Ben, D. H., Romesh, K., and Paul, T. C.: Primary Sulfates in Atmospheric Sulfates: Estimation by
383 Oxygen Isotope Ratio Measurements, *Science*, 217, 51-53, <https://doi.org/10.1126/science.217.4554.51>,
384 1982.
- 385 Brüggemann, M., Riva, M., Perrier, S., Poulain, L., George, C., and Herrmann, H.: Overestimation of
386 Monoterpene Organosulfate Abundance in Aerosol Particles by Sampling in the Presence of SO₂,
387 *Environ. Sci. Technol. Lett.*, 8, 206–211, <https://doi.org/10.1021/acs.estlett.0c00814>, 2021.
- 388 Cheng, Y., Zheng, G., Wei, C., Mu, Q., Zheng, B., Wang, Z., Gao, M., Zhang, Q., He, K., Carmichael,
389 G., Pöschl, U., and Su, H.: Reactive Nitrogen Chemistry in Aerosol Water as a Source of Sulfate during
390 Haze Events in China, *Sci. Adv.*, 2, e1601530, <https://doi.org/10.1126/sciadv.1601530>, 2016.
- 391 Gao, J., Wei, Y., Zhao, H., Liang, D., Feng, Y., and Shi, G.: The role of source emissions in sulfate
392 formation pathways based on chemical thermodynamics and kinetics model, *Sci. Total. Environ.*, 851,
393 158104, <https://doi.org/10.1016/j.scitotenv.2022.158104>, 2022.
- 394 Guo, Z. B., Shi, L., Chen, S. L., Jiang, W. J., Wei, Y., Rui, M. L., and Zeng, G.: Sulfur isotopic
395 fractionation and source apportionment of PM_{2.5} in Nanjing region around the second session of the
396 Youth Olympic Games, *Atmos. Res.*, 174-175, 9-17, <https://doi.org/10.1016/j.atmosres.2016.01.011>,
397 2016.
- 398 Guo, Z., Guo, Q., Chen, S., Zhu, B., Zhang, Y., Yu, J., and Guo, Z. B.: Study on pollution behavior and
399 sulfate formation during the typical haze event in Nanjing with water soluble inorganic ions and sulfur
400 isotopes, *Atmos. Res.*, 217, 198-207, <https://doi.org/10.1016/j.atmosres.2018.11.009>, 2019.
- 401 Han, X., Guo, Q., Liu, C., Fu, P., Strauss, H., Yang, J., Jian, H., Wei, L., Hong, R., Peters, M., Wei, R.,
402 and Tian, L.: Using stable isotopes to trace sources and formation processes of sulfate aerosols from
403 Beijing, China, *Sci. Rep.*, 6, 29958, <https://doi.org/10.1038/srep29958>, 2016.
- 404 Han, X., Guo, Q., Strauss, H., Liu, C., Hu, J., Guo, Z., Wei, R., Peters, M., Tian, L., and Kong, J.:
405 Multiple Sulfur Isotope Constraints on Sources and Formation Processes of Sulfate in Beijing PM_{2.5}
406 Aerosol, *Environ. Sci. Technol.*, 51, 7794-7803, <https://doi.org/10.1021/acs.est.7b00280>, 2017.



407 Harris, E., Sinha, B., Hoppe, P., and Ono, S.: High-precision measurements of ^{33}S and ^{34}S fractionation
408 during SO_2 oxidation reveal causes of seasonality in SO_2 and sulfate isotopic composition, *Environ. Sci.*
409 *Technol.*, 47, 12174-12183, <https://doi.org/10.1021/es402824c>, 2013.

410 Harris, E., Sinha, B., Hoppe, P., Crowley, J. N., Ono, S., and Foley, S.: Sulfur isotope fractionation
411 during oxidation of sulfur dioxide: gas-phase oxidation by OH radicals and aqueous oxidation by H_2O_2 ,
412 O_3 and iron catalysis, *Atmos. Chem. Phys.*, 12, 407-424, <https://doi.org/10.5194/acp-12-407-2012>,
413 2012.

414 He, P. Z., Alexander, B., Geng, L., Chi, X. Y., Fan, S. D., Zhan, H. C., Kang, H., Zheng, G. J., Cheng, Y.
415 F., Su, H., Liu, C., and Xie, Z. Q.: Isotopic constraints on heterogeneous sulfate production in Beijing
416 haze, *Atmos. Chem. Phys.*, 18, 5515–5528, <https://doi.org/10.5194/acp-18-5515-2018>, 2018.

417 He, X., Wu, J. J., Ma, Z. C., Xi, X., and Zhang, Y. H.: NH_3 -promoted heterogeneous reaction of SO_2 to
418 sulfate on $\alpha\text{-Fe}_2\text{O}_3$ particles with coexistence of NO_2 under different relative humidities, *Atmos.*
419 *Environ.*, 262, 118622, <https://doi.org/10.1016/j.atmosenv.2021.118622>, 2021.

420 Huang, R. J., Zhang, Y., Bozzetti, C., Ho, K. F., Cao, J. J., Han, Y., Daellenbach, K. R., Slowik, J. G.,
421 Platt, S. M., Canonaco, F., Zotter, P., Wolf, R., Pieber, S. M., Bruns, E. A., Crippa, M., Ciarelli, G.,
422 Piazzalunga, A., Schwikowski, M., Abbaszade, G., Schnelle-Kreis, J., Zimmermann, R., An, Z., Szidat,
423 S., Baltensperger, U., El Haddad, I., and Prevot, A. S.: High secondary aerosol contribution to
424 particulate pollution during haze events in China, *Nature*, 514, 218–222,
425 <https://doi.org/10.1038/nature13774>, 2014.

426 Kuang, B., Zhang, F., Shen, J., Shen, Y., Qu, F., Jin, L., Tang, Q., Tian, X., and Wang, Z.: Chemical
427 characterization, formation mechanisms and source apportionment of $\text{PM}_{2.5}$ in north Zhejiang Province:
428 The importance of secondary formation and vehicle emission, *Sci. Total. Environ.*, 851, 158206,
429 <https://doi.org/10.1016/j.scitotenv.2022.158206>, 2022.

430 Li, J., Zhang, Y., Cao, F., Zhang, W., and Michalski, G.: Stable Sulfur Isotopes Revealed a Major Role
431 of Transition-Metal Ion-Catalyzed SO_2 Oxidation in Haze Episodes, *Environ. Sci. Technol.*, 54,
432 2626-2634, <https://doi.org/10.1021/acs.est.9b07150>, 2020.

433 Lin, Y. C., Yu, M., Xie, F., and Zhang, Y.: Anthropogenic Emission Sources of Sulfate Aerosols in
434 Hangzhou, East China: Insights from Isotope Techniques with Consideration of Fractionation Effects
435 between Gas-to-Particle Transformations, *Environ. Sci. Technol.*, 56, 3905-3914.



- 436 <https://doi.org/10.1021/acs.est.1c05823>, 2022.
- 437 Liu, M. X., Song, Y., Zhou, T., Xu, Z. Y., Yan, C. Q., Zheng, M., Wu, Z. J., Hu, M., Wu, Y. S., and Zhu,
438 T.: Fine particle pH during severe haze episodes in northern China, *Geophys. Res. Lett.*, 44,
439 5213–5221, <https://doi.org/10.1002/2017GL073210>, 2017.
- 440 Liu, T., Clegg, S. L., and Abbatt, J. P. D.: Fast oxidation of sulfur dioxide by hydrogen peroxide in
441 deliquesced aerosol particles, *Proc. Natl Acad. Sci. USA.*, 117, 1354–1359,
442 <https://doi.org/10.1073/pnas.1916401117>, 2020.
- 443 Liu, Y. Y., Wang, T., Fang, X. Z., Deng, Y., Cheng, H. Y., Nabi, I., and Zhang, L.: Brown carbon: An
444 underlying driving force for rapid atmospheric sulfate formation and haze event, *Sci. Total. Environ.*,
445 734, 139415, <https://doi.org/10.1016/j.scitotenv.2020.139415>, 2020.
- 446 Meng, X., Hang, Y., Lin, X., Li, T. T., Wang, T. J., Cao, J. J., Fu, Q. Y., Dey, S., Huang, K., Liang, F. C.,
447 Kan, H. D., Shi, X. M., and Liu, Y.: A satellite-driven model to estimate long-term particulate sulfate
448 levels and attributable mortality burden in China, *Environ. Int.*, 171, 107740,
449 <https://doi.org/10.1016/j.envint.2023.107740>, 2023.
- 450 Oh, S. H., Park, K., Park, M., Song, M., Jang, K. S., Schauer, J. J., Bae, G. N., and Bae, M. S.:
451 Comparison of the sources and oxidative potential of PM_{2.5} during winter time in large cities in China
452 and South Korea, *Sci. Total. Environ.*, 859, 160369, <https://doi.org/10.1016/j.scitotenv.2022.160369>,
453 2023.
- 454 Ramanathan, V., Crutzen, P. J., Kiehl, J. T., and Rosenfeld, D.: Aerosols, climate, and the hydrological
455 cycle, *Science*, 294, 2119–2124, <https://doi.org/10.1126/science.1064034>, 2001.
- 456 Seinfeld, J. H. and Pandis, S. N.: Atmospheric Chemistry and Physics: From Air Pollution to Climate
457 Change, *Phys. Today*, 51, 88–90, <https://doi.org/10.1063/1.882420>, 1998.
- 458 Shao, J., Chen, Q., Wang, Y., Lu, X., He, P., Sun, Y., Shah, V., Martin, R. V., Philip, S., Song, S., Zhao,
459 Y., Xie, Z., Zhang, L., and Alexander, B.: Heterogeneous sulfate aerosol formation mechanisms during
460 wintertime Chinese haze events: air quality model assessment using observations of sulfate oxygen
461 isotopes in Beijing, *Atmos. Chem. Phys.*, 19, 6107–6123, <https://doi.org/10.5194/acp-19-6107-2019>,
462 2019.
- 463 Tanaka, N., Rye, D. M., Xiao, Y., and Lassaga, A. C.: Use of stable sulfur isotope systematic for
464 evaluating oxidation reaction pathways and in-cloud scavenging of sulfur dioxide in the atmosphere,



- 465 Geophys. Res. Lett., 21, 1519-1522, <https://doi.org/10.1029/94GL00893>, 1994.
- 466 Wang, G. H., Zhang, R. Y., Gomez, M. E., Yang, L. X., Levy Zamora, M., Hu, M., Lin, Y., Peng, J. F.,
467 Guo, S., Meng, J. J., Li, J. J., Cheng, C. L., Hu, T. F., Ren, Y. Q., Wang, Y. S., Gao, J., Cao, J. J., An, Z.
468 S., Zhou, W. J., Li, G. H., Wang, J. Y., Tian, P. F., Marrero-Ortiz, W., Secretst, J., Du, Z. F., Zheng, J.,
469 Shang, D. J., Zeng, L. M., Shao, M., Wang, W. G., Huang, Y., Wang, Y., Zhu, Y. J., Li, Y. X., Hu, J. X.,
470 Pan, B., Cai, L., Cheng, Y. T., Ji, Y. M., Zhang, F., Rosenfeld, D., Liss, P. S., Duce, R. A., Kolb, C. E.,
471 and Molina, M. J.: Persistent sulfate formation from London Fog to Chinese haze, Proc. Natl. Acad. Sci.
472 U.S. A., 113, 13630-13635, <https://doi.org/10.1073/pnas.1616540113>, 2016.
- 473 Wang, W., Liu, M., Wang, T., Song, Y., and Ge, M.: Sulfate formation is dominated by
474 manganese-catalyzed oxidation of SO₂ on aerosol surfaces during haze events, Nature Communications,
475 12, 1993, <https://doi.org/10.1038/s41467-021-22091-6>, 2021.
- 476 Xue, J., Yuan, Z., Griffith, S. M., Yu, X., Lau, A. K. H., and Yu, J. Z.: Sulfate Formation Enhanced by a
477 Cocktail of High NO_x, SO₂, Particulate Matter, and Droplet pH during Haze-Fog Events in Megacities
478 in China: An Observation-Based Modeling Investigation, Environ. Sci. Technol., 50, 7325–7334,
479 <https://doi.org/10.1021/acs.est.6b00768>, 2016.
- 480 Xue, J., Yuan, Z., Yu, J. Z., and Lau, A. K. H.: An Observation-Based Model for Secondary Inorganic
481 Aerosols, Aerosol Air Qual. Res., 14, 862–878, <https://doi.org/10.4209/aaqr.2013.06.0188>, 2014.
- 482 Yang, T., Xu, Y., Ye, Q., Ma, Y. J., Wang, Y. C., Yu, J. Z., Duan, Y. S., Li, C. X., Xiao, H. W., Li, Z. Y.,
483 Zhao, Y., and Xiao, H. Y.: Spatial and diurnal variations of aerosol organosulfates in summertime
484 Shanghai, China: potential influence of photochemical processes and anthropogenic sulfate pollution,
485 Atmos. Chem. Phys., 23, 13433–13450, <https://doi.org/10.5194/acp-23-13433-2023>, 2023.
- 486 Ye, C., Liu, P. F., Ma, Z. B., Xue, C. Y., Zhang, C. L., Zhang, Y. Y., Liu, J. F., Liu, C. T., Sun, X., and
487 Mu, Y. J.: High H₂O₂ Concentrations Observed during Haze Periods during the Winter in Beijing:
488 Importance of H₂O₂ Oxidation in Sulfate Formation, Environ. Sci. Technol. Lett., 5, 757-763,
489 <https://doi.org/10.1021/acs.estlett.8b00579>, 2018.
- 490 Zhang, R., Sun, X. S., Shi, A. J., Huang, Y. H., Yan, J., Nie, T., Yan, X., and Li, X.: Secondary
491 inorganic aerosols formation during haze episodes at an urban site in Beijing, China, Atmos. Environ.,
492 177, 275-282, <https://doi.org/10.1016/j.jes.2022.01.008>, 2018.
- 493 Zhang, Y., Bao, F., Li, M., Xia, H., and Zhao, J.: Photoinduced Uptake and Oxidation of SO₂ on Beijing

<https://doi.org/10.5194/egusphere-2023-2554>
Preprint. Discussion started: 20 November 2023
© Author(s) 2023. CC BY 4.0 License.



494 Urban PM_{2,5}, Environ. Sci. Technol., 54, 14868-14876, <https://doi.org/10.1021/acs.est.0c01532>, 2020.